

Electrical Transport Properties of Some Sodium Silicate Glasses Containing By-Pass Cement Dust

A.M. Abdel-Ghany¹, A.A. Bendary², T.Z. Abou-El-Nasr², M.Y. Hassaan² and A.G. Mostafa^{2*}

¹ Department of Basic Science, Faculty of Engineering Science, Sinai University, El-Arish, Egypt

² Department of Physics, Faculty of Science, Al-Azhar University, Nasr City, Cairo, Egypt

*drahmedgamal@yahoo.com

Abstract: Some sodium-silicate glasses containing different amounts of by-pass cement dust (BCD) were prepared by the melt quenching method. The selected molecular composition was [(70-x)% SiO₂-x% BCD-30% Na₂O (x = 15, 20, 25, 30 and 35)]. The experimental density and molar volume were studied and were then compared with the empirically calculated values (the close packed structure). The comparison evidenced the short range order of the studied glass samples. The electric and dielectric properties were thoroughly investigated. The appearance of a maxima and minima in the total conductivity of the BCD concentration dependence was attributed to the mixed alkali effect as well as to the presence of a considerable amount of CaO. It was concluded also that all glasses behave like semiconductors. The Cole-Cole diagrams indicated a single relaxation process and the Cole-Cole distribution parameters (α) indicated that all samples are of high homogeneity.

[Abdel-Ghany AM, Bendary AA, Abou-El-Nasr TZ, Hassaan MY and Mostafa AG. **Electrical Transport Properties of Some Sodium Silicate Glasses Containing By-Pass Cement Dust.** *Nat Sci* 2014;12(6):139-147]. (ISSN: 1545-0740). <http://www.sciencepub.net/nature>. 20

Keywords: By-pass Cement Dust; Silicate glasses; Electrical Transport Properties.

1. Introduction

Cement industry is a matter of necessity in our daily life now, since cement has been usually needed to construct all buildings. Therefore cement factories are widely spread here and there over the world [1]. Such industry is also accompanied with a dangerous type of waste which is the by-pass cement dust (BCD). This waste is usually accumulated in huge amounts and it causes various diseases, especially those related to human respiratory system. The chemical analysis of such waste indicated that, it contains various oxides, mainly, CaO, SiO₂, Na₂O, Al₂O₃, K₂O and Fe₂O₃ [2], where all these oxides can be usually used for manufacturing various types of glasses [3].

On the other hand, amorphous materials and glasses appear now of interest due to their functional applications in both science and technology [4]. For example, silicate glasses play an important role in several fields of glass manufacture, like for instance, glasses for commercial uses as well as micro-electronic device technology. Therefore much effort has been devoted during the last few years to produce high purity samples, eventually doped with a controlled amount of impurities [5-6]. In many scientific applications, some glasses can be used as electrical insulators while some others can be used as conductors. Therefore, the understanding of the electrical conductivity of glasses is very important. Generally, traditional commercial silicate glasses are poor conductors, but the electrical conduction in silicate glasses contain alkali oxide is usually caused by the ionic motion in the glass network [7]. It is

known also that the amount and type of the alkali oxide introduced in a glass network make fundamental relation with several properties of such glass [5, 8-10]. Although a great deal of work has been done to determine the electrical conductivity in such like glasses, more work is still needed to clarify the true mechanism of conduction [5].

However it will be tried to prepare some silicate glasses with additives of BCD in different proportions aiming to consume the waste accumulation as well as to obtain cheaper glasses. The obtained solid glass will be thoroughly investigated from the electrical properties point of view.

2. Experimental

The BCD was supplied by Sinai Cement Co., El-Arish, Egypt, and it was analyzed using X-ray fluorescence apparatus model (PANalytical Axios advanced, Netherlands). The obtained chemical analysis is exhibited in Table (1).

The selected glass batches were weighted from pure sodium carbonate, silicon oxide and the supplied BCD, so that, when melted, they give glasses having the following percentage molecular composition (70-x) SiO₂-30 Na₂O-x BCD, where x= 15, 20, 25, 30 and 35. The weighted batches were ground and mixed well using an agate mortar, and they were melted in porcelain crucibles in an electric muffle furnace for 2 hrs at 1450K. The melts were stirred several times during melting, and they were then poured between two copper plates in air. The obtained glass samples, just after solidifying, were

transferred to the annealing furnace at 600K for 2 hrs. Then the furnace was turned off and left to cool to RT overnight, with a cooling rate of 0.42 K/min.

The experimental density was measured applying Archimedes technique, using CCl_4 as an immersion liquid, applying equation (1),

$$\rho_{\text{exp}} = \left[\frac{M_a}{M_a - M_l} \right] \rho_l \quad (1)$$

where ρ_{exp} is the density of a sample, M_a is the mass of the sample in air, ρ_l is the density of liquid and M_l is the mass of sample in liquid.

The molar volume values were then calculated from equations (2) [11-12].

$$(V_m)_{\text{exp}} = \sum (M_i / \rho_{\text{exp}}) \quad (2)$$

where M_i is the molecular weight in (g/mol) of a sample and ρ_{exp} is the experimental density value of such sample.

The empirical density values were also calculated using equation (3),

$$\rho_{\text{emp}} = \sum X_i \rho_i \quad (3)$$

where ρ_i are the densities of the oxides forming the glass, X_i is the mole fraction of each oxide. The empirical molar volume values were then calculated using equation (4) [13-14].

$$(V_m)_{\text{emp}} = \sum (M_i / \rho_{\text{emp}}) \quad (4)$$

where M_i is the molecular weight in (g/mol) and ρ_{emp} is the calculated densities of the close packed structure of the corresponding material.

For electrical measurements, the obtained glasses were polished from both sides in order to obtain disk shape samples of 8 mm diameter and 2 mm thickness. Then the disks were coated from both sides with an air drying silver paste to achieve good electrical contact. The measurements were carried out using a computerized Stanford LCR bridge model SR 720 at four fixed frequencies [0.12, 1, 10, 100 kHz], and all measurements were performed in the temperature range from 300 to 600K.

Table 1. The chemical analysis of the BCD.

Constituting oxides	CaO	SiO ₂	Na ₂ O	Fe ₂ O ₃	MgO	K ₂ O	Al ₂ O ₃	Cl ⁻	SO ₃	LOI*
Relative amounts (%)	60.12	17.06	1.59	2.46	1.2	4.81	4.64	2.9	0.95	4.37

*LOI is loss of ignition

3. Results and Discussion

The amorphous nature of the prepared samples was examined visually and by touch. For more conformation, the density of the studied glasses was measured experimentally applying the liquid displacement technique and the obtained values were compared with those obtained theoretically for the close packed structure of the corresponding compositions.

Both the experimental and empirical density values were plotted in Fig. (1) as a function of BCD content, for comparison. It can be seen that both density values (empirical and experimental) increased gradually and linearly with the gradual increase of BCD. It is observed also that the empirical density is usually higher than the corresponding experimental density. On the other hand, since the molar volume is directly related to the internal spatial structure of materials, it is suitable to exhibit also the molar volume values of the studied glasses [11]. Fig. (2) exhibits the calculated molar volume values (of both the empirical and experimental calculations). They show a linear gradual decrease as the BCD content

was gradually increased. It is observed also that the empirical values are usually lower than these obtained experimentally.

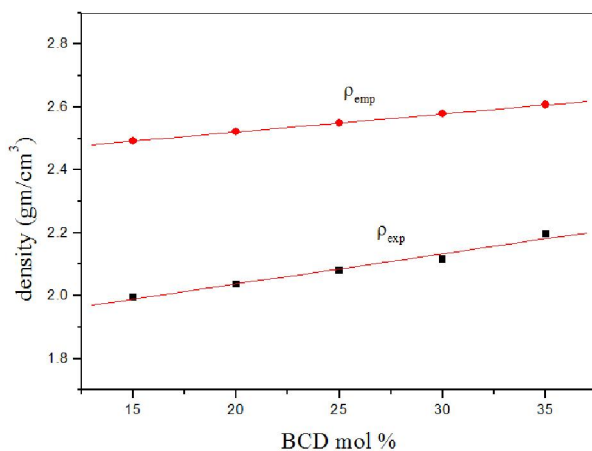


Figure 1. The change in density as function of BCD content.

Also, the rate of the decrease of the experimental molar volume values appeared to be higher than that of the corresponding empirical rate of change. The observed decrease of both the empirical and the experimental molar volume may be due to:

- i- The BCD contains various positive cations, where these cations fill mostly the network vacancies, and in turn decreases the internal free volume.
- ii- The decrease in the oxygen ion densities in the glass networks as the BCD was gradually introduced replacing SiO_2 .

Accordingly the density is logically increased, while the molar volume is gradually decreased, as BCD was gradually increased.

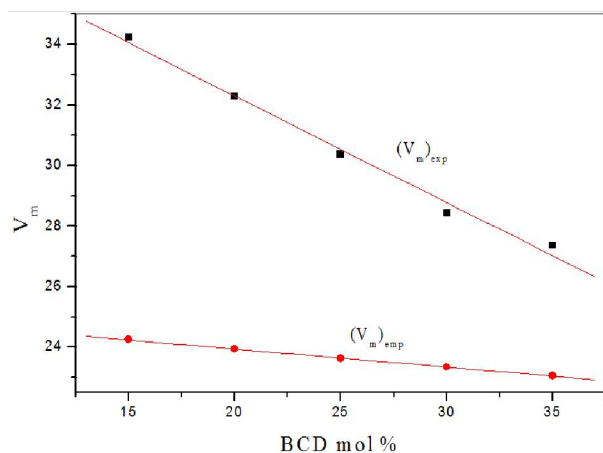


Figure 2. The change in molar volume as a function of BCD content.

The higher empirical density as well as the lower empirical molar volume in comparison to the corresponding experimental values can be taken as evidences for the amorphous nature and the short range order of the studied glass samples. Accordingly, the glassy nature of the studied samples was thus confirmed, and it is worth to state that it was not easy to obtain pure glasses with higher amounts of BCD more than 35 mol%, while no limits for the lower amounts.

Since the studied samples are confirmed to be glasses, hence the frequency dependence of the total conductivity ($\sigma_{(\omega,T)}$) for all samples must follows equation number (5),

$$\sigma_{(t)} = \sigma_{dc} + A\omega^s \quad (5)$$

where σ_{dc} is the frequency independent conductivity, A is a weakly temperature dependent factor, s is the exponent factor and ω is the angular frequency [15-16]. The obtained experimental data of the temperature dependence total conductivity ($\sigma_{(t)}$) for

sample no. (2) (as a representative figure), are exhibited in Fig. (3) as a function of $1000/T$. It is appeared that at low temperatures the conductivity shows weak temperature dependence and strong frequency dispersion, while at high temperatures $\sigma_{(t)}$ shows strong temperature dependence and weak frequency dependence. It was found that all sample exhibited similar behavior. From these observation it can be stated that, the dc conductivity is dominant at high temperatures and the ac conductivity is dominant at low temperatures. It is concluded also that, from the conductivity values that all samples behave like semiconductors.

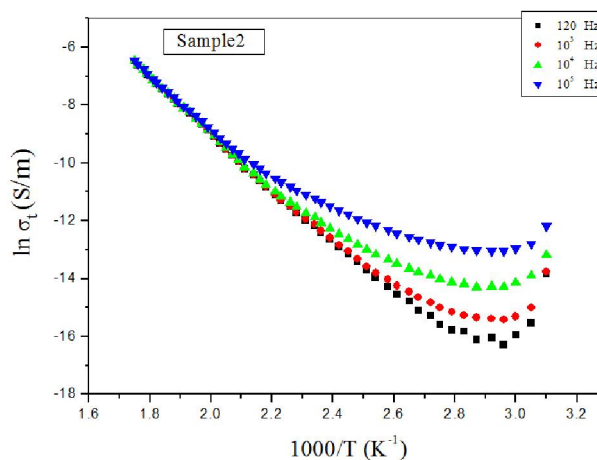


Figure 3. Temperature dependence of the total conductivity for sample no. (2) as a representative figure.

Fig. (4), shows the variation of $\ln\sigma_t$ as a function of BCD content. Since the BCD consists of 60% CaO , 1.59% of Na_2O and 4.81% of K_2O , it is supposed that an electrical resistance interaction between the alkali and the alkaline earth cations occurs. Interesting physical effects have been previously observed in studying the behavior of glassy ionic conductors by Mansour [17]. The understanding of the microscopic mechanism for ion conduction in glass is a longstanding problem in glass science. Many glasses exhibit a roughly linear behavior with changing their chemical composition. But glasses containing two different alkali oxides are a major exception to this trend due to the mixed alkali effect (MAE) phenomenon [17]. For the studied glasses, the deviation from linearity may be so great that maxima and minima occur. Moreover, the MAE was observed as a dramatic non-linear trend due to the introduction of alkali and alkaline earth cations, where the resistance increased with increasing the difference between the radii of the alkali and alkaline earth cations [17-18].

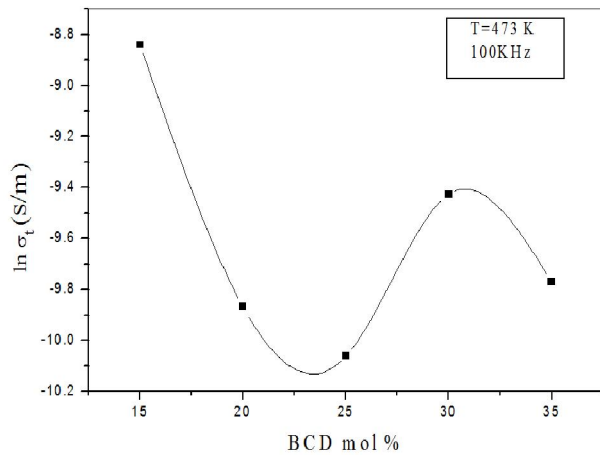


Figure 4. The total conductivity as a function of BCD content.

At temperature (370 K) the relation between $\ln(\sigma_t)$ and $\ln(\omega)$ for sample no.(2), is shown in Fig. (5) (as a representative figure).

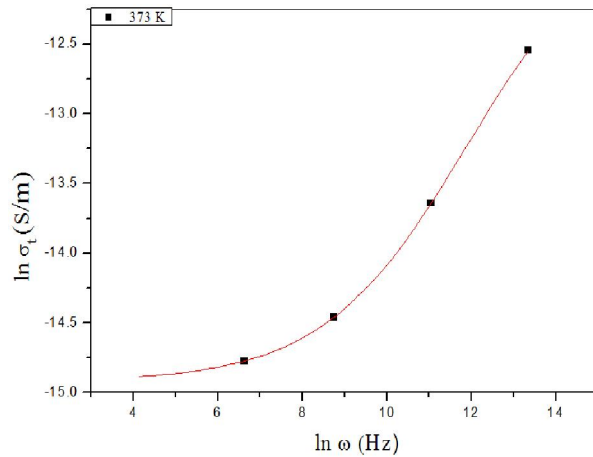


Figure 5. $\ln\sigma_t$ versus $\ln\omega$ at a fixed temperate.

The dots and solid line represent the experimental data and the theoretical fitting respectively. It can be seen that, at low frequency the conductivity is fixed and approximately independent of frequency, while at high frequency the conductivity increased [19], and all samples exhibit similar behavior. The experimental values of the dc conductivity (black points) and the fitting of equation (5) are plotted in Fig. (6) as a function of the concentration of BCD, where it shows approximately the same behavior, like that of the total conductivity.

The activation energy of the dc conductivity can be calculated form the slopes of the obtained straight lines of the studied sample according to Arrhenius equation (equation number 6) at high

temperatures, where the dc conductivity is only the dominant.

$$\sigma_{dc} = \sigma_0 \exp(-\Delta E/kT) \tag{6}$$

where σ_0 is the pre-exponential factor and ΔE is the activation energy. The variation of the activation energy with the variation of BCD is exhibited in Fig. (7), where this figure shows approximately the reverse behavior of the conductivity [20-21], and such trend was expected as s logic result.

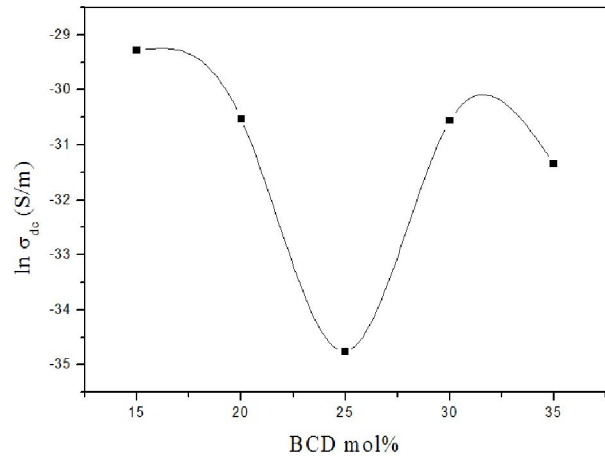


Figure 6. The dc conductivity as a function of BCD content.

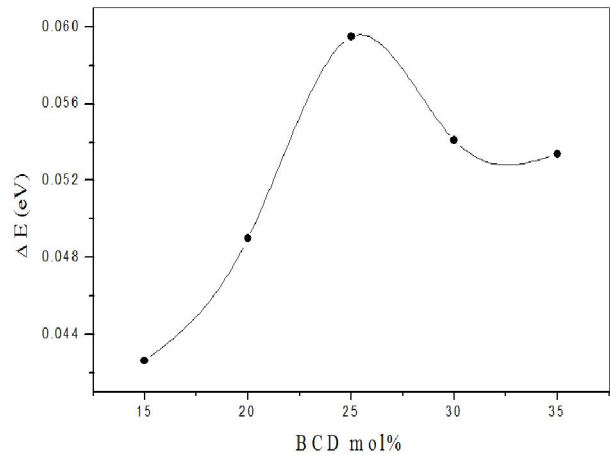


Figure 7. The dc activation energy as a function of BCD content.

Fig. (8), shows the variation of the s-factor as a function of temperature for sample no. (2), (as a representative figure). The obtained values of the exponent factor (s), for all samples, show a gradual decrease with the increase of temperature. Because of the agreement between the experimental behavior of

the exponent factor(s) and those predicted by the CBH model (equation (7)), proposed by Elliot [22], it is supposed that such model can be used to describe the conduction mechanism in these glasses, and it is observed that, all samples exhibit the same behavior.

$$S = 1 - \frac{6kT}{W_m - kT \ln(\omega\tau_0)} \quad (7)$$

where ($\tau_0 = f_0^{-1}$) is the characteristic relaxation time in between 10^{-9} and 10^{-12} sec, k is the Boltzman constant, T is the absolute temperature and W_m is the energy required to remove an electron from its site to infinity.

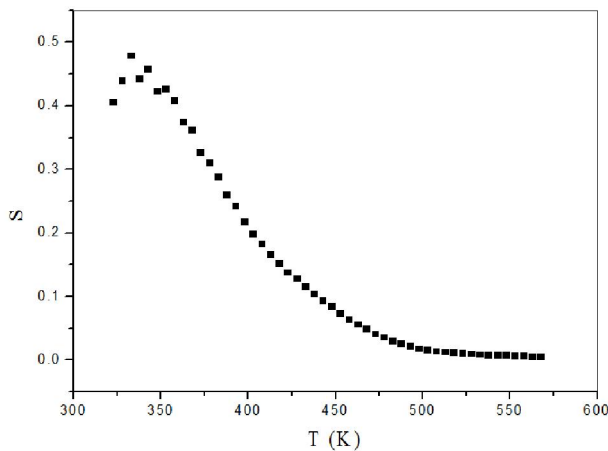


Figure 8. S-factor as a function of temperature for sample (2) as representative figure.

The dielectric constant (ϵ') has been measured, and Fig. (9) shows the variation of ϵ' as a function of T for sample no. (2), (as a representative figure). It was observed that at low temperatures ϵ' is almost independent of temperature and show weak frequency dispersion, while at high temperatures it increases gradually as the temperature was increased, but it shows an inverse variation with frequency. The reason for this behavior is that, the electric dipoles move almost parallel to the ac external electric field and create an inverse internal electric field. With the increase of temperature the movement of the electric dipole is easier and the dipoles move parallel to the ac external electric field and then the internal electric field increased and acts to decrease the dielectric constant [23-24]. It is also found that all samples exhibited similar behavior.

On the other hand, Fig. (10), shows the variation of the dielectric loss factor (ϵ'') as a function of temperature for sample no. (2) (as a representative figure). It is clear that at low temperatures ϵ'' exhibit approximately stable value, while at high

temperatures it starts to increase as the temperature was increased, such that the increment rate is inversely proportional to the frequency. This behavior was explained by Stevels [23-24] who divided the relaxation phenomena into three parts, the conduction loss, the dipole loss and the vibrational loss. Since the conduction loss is proportional to $\sigma(\omega)$, therefore ϵ'' increases as the conductivity increased, where $\sigma(\omega)$ is temperature dependent quantity.

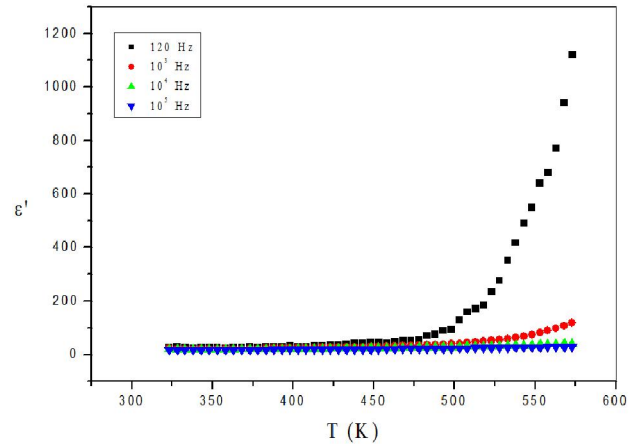


Figure 9. The dielectric constant Temperature dependence at different frequencies.

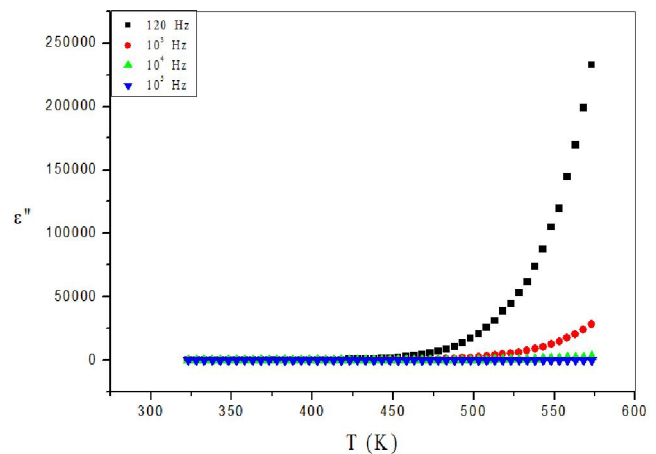


Figure 10. The dielectric loss temperature dependence for sample no. (2) as representative figure.

The dielectric loss factor (ϵ'') as a function of frequency was found to obey a power law of the form [25] (equation (8)),

$$\epsilon'' = B \omega^m \quad (8)$$

where B is a constant. The plot of $\ln(\epsilon'')$ against $\ln(\omega)$ must be a straight line with negative slope (m) as

shown in Fig. (11), for sample no. (2) as a representative figure at 323, 373, 423 and 473K. The value of m as a function of temperature can be described by Guintini equation (9) [25],

$$m = -4kT/W_m \tag{9}$$

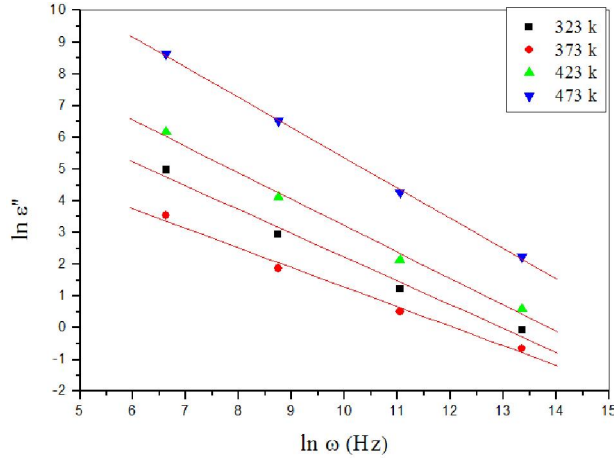


Figure 11. The dielectric loss (ϵ'') as a function of frequency at different temperatures for sample no. (2) as representative figure.

Fig. (12) shows the variation of W_m as a function the BCD content, where the change of W_m shows the reversed behavior of the change $\ln\sigma(t)$ [25-27], which is also a logic result.

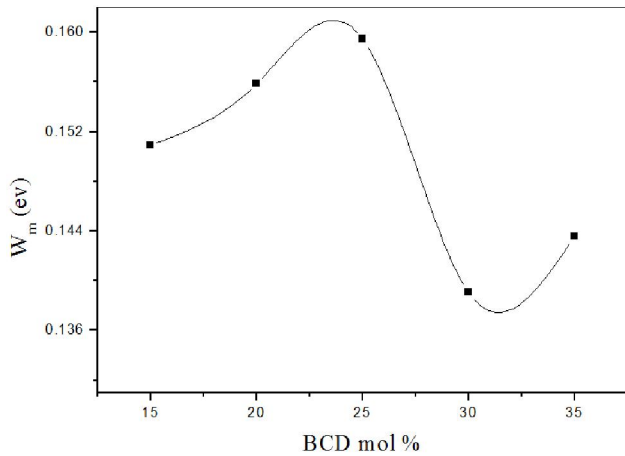


Figure 12. the variation of W_m as a function of BCD at fixed temperature, for sample no. (2) as representative figure.

Cole-Cole diagram (frequency dependence) and pseudo-Cole-Cole diagram (temperature dependence), for a complex dielectric data provides information about the various kinds of relaxation

phenomena as well as the static and dynamic dielectric constants which are crucial values for device fabrication in micro-electronics. However both Cole-Cole diagrams were obtained by plotting the imaginary part of the electric modulus $M''(\omega)$ (equation (10)), against the real part $M'(\omega)$ (equation (11)), at constant temperature [28], where

$$M''(\omega) = \epsilon'' / (\epsilon'^2 + \epsilon''^2) \tag{10}$$

$$M'(\omega) = \epsilon' / (\epsilon'^2 + \epsilon''^2) \tag{11}$$

Fig. (13) show Cole-Cole diagrams at 373K for the investigated glasses, where it shows a single semicircle [29], and all samples exhibited similar behavior.

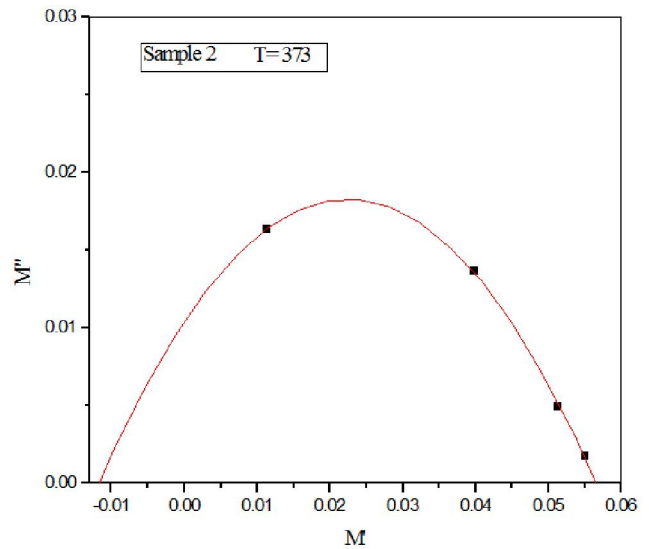


Figure 13. Cole-Cole diagram for sample no. (2), as a representative figure.

Fig. (14) shows the pseudo Cole-Cole diagrams at 100 kHz for the investigated glasses. It is clear that all plots of $M''(T) \sim M'(T)$ show a single semicircle, indicating a single relaxation process with an agreement to that predicted from Cole-Cole diagrams.

From another point of view, both Cole-Cole equations are used to describe both the dielectric constant and the dielectric loss factor [30-31],

$$\epsilon' = \epsilon_\infty + \frac{(\epsilon_0 - \epsilon_\infty)[1 + (\omega\tau)^{(1-a)} \sin(a\pi/2)]}{[1 + 2(\omega\tau)^{(1-a)} \sin(a\pi/2) + (\omega\tau)^{2(1-a)}]} \tag{12}$$

$$\epsilon'' = \frac{(\epsilon_0 - \epsilon_\infty)[1 + (\omega\tau)^{(1-a)} \cos(a\pi/2)]}{[1 + 2(\omega\tau)^{(1-a)} \sin(a\pi/2) + (\omega\tau)^{2(1-a)}]} \tag{13}$$

where ϵ_0 is the static dielectric constant (dc dielectric constant), ϵ_∞ is the optical dielectric constant (the high frequency dielectric constant) and (α) is Cole-Cole distribution parameter which has a value in between 0 and 1, such that the value zero means a single relaxation time. However Cole-Cole equations were used to fit the frequency dependence of both the dielectric constant and the dielectric loss factor. For the studied glasses, the calculated values of the Cole-Cole distribution parameter (α) are exhibited in Table (2) and the obtained values indicated a single relaxation process for all samples. From fitting, the obtained values of α were found to lie between 0.001 and 0.11 which means a single relaxation process for all samples of the studied system [31].

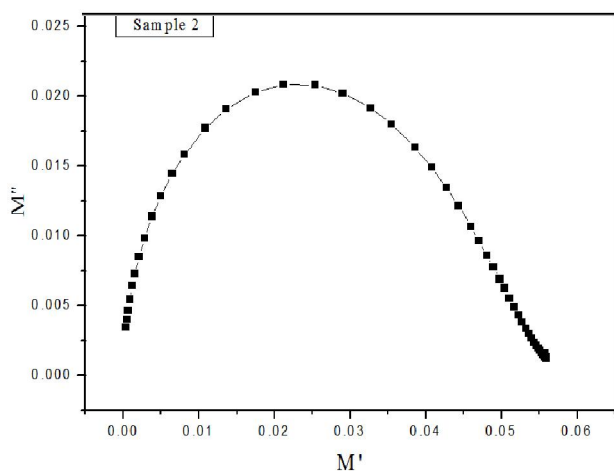


Figure 14. Pseudo Cole-Cole diagram at 100 kHz for sample no. (2), as representative figure.

Table 2. The obtained values of α at 373 K for the studied samples.

BCD conc. %	15	20	25	30	35
α	0.041	0.035	0.091	0.109	0.001

Fig. (15), exhibit the frequency dependence of the dielectric loss factor at 373 K, where the dots represent the experimental data and the solid lines represent their fitting using Cole-Cole equation, and all samples exhibit similar behavior.

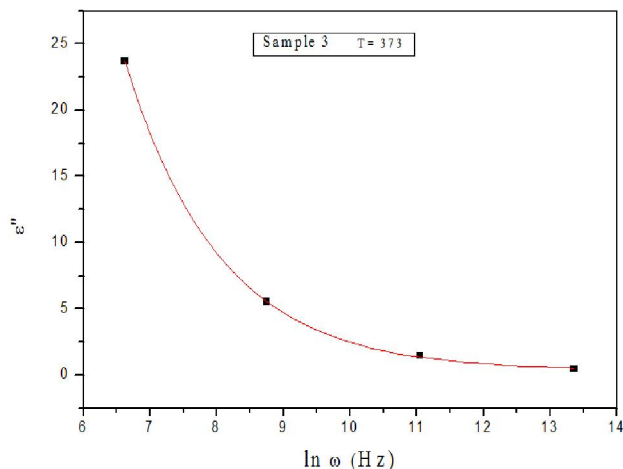


Figure 15. The fitting of ϵ'' values with Cole-Cole equation, for sample no.2, as a representative figure.

Since it is not available to obtain the maximum peak height from the temperature dependence of $\tan(\delta)$, therefore the imaginary modulus (M'') can be applied to calculate the dielectric activation energy of dipole (ΔE_D) by using equation (14).

$$\tau = \tau_0 \exp(\Delta E_D / kT) \tag{14}$$

where ($\tau = \tau^{-1}$) is the relaxation time and ΔE_D the dielectric relaxation activation energy for dipoles [34].

Fig. (16) represents the imaginary modulus (M'') versus temperature at four different frequencies (0.12, 1, 10 and 100 kHz). Generally, for all the studied samples, it is observed that, M'' showed a relaxation peak at a certain temperature (T_m), shifted to higher temperatures as the frequency was increased, indicating the relaxation character of the dielectric loss in the studied glasses [32]. This behavior (relaxation phenomena) can be attributed to the frequency dependence of the orientational polarization [33].

However, Fig. (17) represents the variation of the activation energy of dipoles (ΔE_D) as a function of BCD content, where (ΔE_D) shows also the reverse behavior of that of the conductivity. The larger value of the dielectric relaxation activation energy (ΔE_D) indicates the relaxation mechanism is of the dipolar type [34-35].

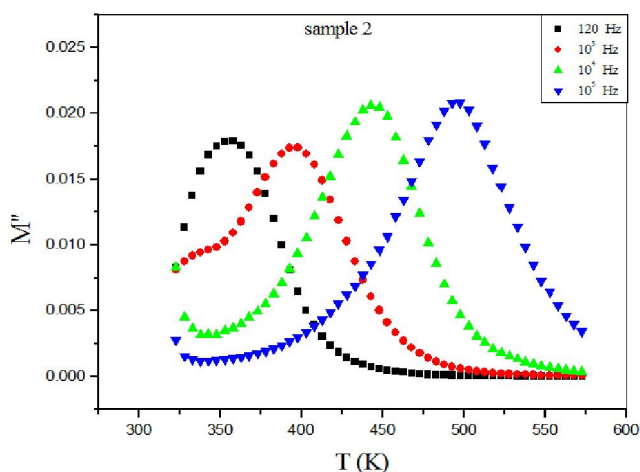


Figure 16. The variation of the imaginary part of the complex electrical modulus (M'') versus temperature at different frequencies.

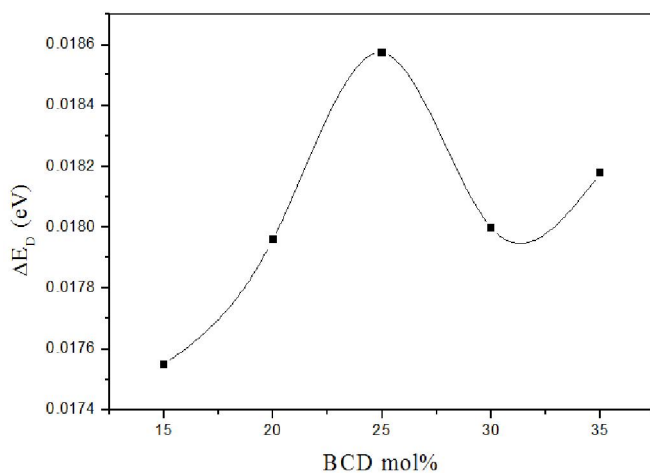


Figure 17. The activation energy of dipole as a function of BCD concentration.

4. Conclusion

It was found that the recycling of the BCD in the glass manufacture is a matter of interest due the accumulation of huge amounts as well as its dangerous attack to the human reparatory system. It was conclude that sodium silicate glasses accept up to 35 mol % to give pure homogenous glasses, which evidenced by comparing the experimental and empirical density and molar volume values. It was concluded also, from studying the electric and dielectric properties that all glasses behave like semiconductors. The mixed alkali effect and the amount of CaO present act to corrupt the expected linear behavior of the total conductivity dependence

BCD concentration. Also, Cole-Cole diagrams evidenced a Debye relaxation phenomenon in all glasses, while Cole-Cole distribution parameter (α) evidenced the homogeneity of all samples.

Acknowledgement:

The authors would like to express their sincere gratitude to Eng./ Shaaban Saied and Eng./ Mohamed Kottb, the big mangers of El-Arish cement Co., for supplying the BCD used in this article.

Corresponding Author:

Dr. Ahmed G. Mostafa
Department of Physics
Faculty of Science
Al-Azhar University, Nasr City, Cairo, Egypt
E-mail: drahmedgamal@yahoo.com

References

1. F. M. E. Misilhy, Ph.D. Thesis, Phys. Dept, Faculty of Science, AL-Azhar Univ., Egypt, (2006).
2. S. Grandi, P. Mustarelli, A. Magistris, M. Gallorini and E. Rizzio, *J. Non-Cryst. Solids*, 303 (2002) 208.
3. A. Feltri, S. Grandi, P. Mustarelli, M. Cutroni and A. Mandanici, *J. Solid State Ionics*, 154 – 155 (2002) 217.
4. G. Robert, J. P. Malugani and A. Saida, *Solid State Ionics*, 5 (1981) 311.
5. I. F. Kelly, T. F. Cordaro and M. Tomazawa, *J. Non-Cryst. Solids*, 31 (1980) 47.
6. Y. M. Han, N. I. Kreidle and D. E. Day, *J. Non-Cryst. Solids*, 30 (1979) 241.
7. S.W. Martin, *J. Am. Ceram. Society*, 71 (1988) 438.
8. M. Ribes, D. Ravaine, J.L. Souquet and M. I. Mourin, *Rev. Chim. Miner.*, 16 (1979) 339.
9. R. Mercier, J.P. Malugani, B. Fahys, and G. Robert, *Solid State Ionics*, 5 (1981) 663.
10. M. Wada, M. Mcnetrier, A. Le Vasseur and P. Hagenmuller, *Mater. Res.Bull.*, 18 (1983) 189.
11. H. Mori, H. Matsuno and H. Sakata, *J. Non-Cryst Solids*, 276 (2000) 78.
12. S. Duhan, S. Sanghi, A. Agarwal, A. Sheoran and S. Rani, *Physica B*, 404 (2009) 1648.
13. T. Takada, S. F. Wang, S. Yoshikawa, S. J. Jang and R. E. Newnham: *J. Am. Ceram. Soc.*, 77 (1994) 1909.
14. S. Wuy, X. Wei, X. Wang, H. Yang and H. Gao, *J. Mater. Sci. & Technol.*, 26 (5) (2010) 472.

15. P. Muralidharan, M. Venkateshwarlu and N. Satyanarayana, *J. Non-Cryst. Solids*, 351(2005) 583.
16. K. Otto, *Phys. Chem. Glasses*, 7 (1) (1966) 29.
17. E. Mansour, *Physica B*, 362 (2005) 88.
18. D. E. Day, *J. Non-Cryst. Solids*, 21 (1976) 343.
19. A. M. Abdel-Ghany, Ph. D. Thesis, Phys. Dept., Faculty of science AL-Azhar Univ., (2011).
20. G. D. L. K. Jayasinghe, M. A. K. L. Dissanayake, P. W. S. K. Bandaranayake, J. L. Souquet and D. Foscallo, *Solid State Ionics*, 121 (1999) 19.
21. R. Elliot, *Adv. Phys.*, 18 (1987) 31.
22. S. S. Fouad, A. E. Bekheet and A. M. Farid, *Physica B*, 322 (2002) 163.
23. S. R. Elliott, *Phil. Mag. B*, 36 (1978) 1291.
24. K. Shimakawa, *Phil. Mag.*, 46 (1982) 123.
25. J. C. Giantini and J. V. Zancheha, *J. Non-Cryst. Solids*, 34 (1979) 419.
26. J. C. Pilet and A. Leraon, *Advances in molecular relaxation*, 14 (1979) 235.
27. L. Murawski and R. J. Barczyn 'ski, *J. Solid State Ionics*, 176 (2005) 2145.
28. A. Mogus-Milankovic, B. Santic, C. S. Ray and D. E. Day, *J. Non-Cryst. Solids*, 263 & 264 (2000) 299.
29. A. S. Reo, Y. N. Ahammed, R. R. Reddy and T. V. R. Reo, *J. Optics Materials*, 10 (1998) 245.
30. R. Murugaraj, *J. Materials Science*, 42 (24) (2007) 10065.
31. J. K. Lee, H. W. Park, H. W. Choi, J. E. Kim, S. J. Kim and Y. S. Yang, *J. Korean Physical Society*, 47 (2005) 267.
32. Y. Dimitriv, V. Dimitrov, M. Arnaudov and D. Topalov, *J. Non-Cryst. Solids*, 57 (1983) 147.
33. S. Kumar, M. Husain and M. Zulfequar, *Physica B*, 387 (2007) 400.
34. A. G. Mostafa, F. Abdel-Wahab and G. A. Yahya, *J. Material Science: Material in Electronics*, 13 (2002) 721.
35. D. K. Durga and N. Veeraiah, *Physica B*, 324 (2002) 127.

6/14/2014